

Iterative Cross-Scanner Registration for Whole Slide Images

Luisa Theelke*

Pattern Recognition Lab, Computer Sciences
Friedrich-Alexander-Universität
Erlangen-Nürnberg, Germany

`luisa.theelke@fau.de`

Christian Marzahl

Pattern Recognition Lab, Computer Sciences
Friedrich-Alexander-Universität
Erlangen-Nürnberg, Germany

`christian.marzahl@fau.de`

Robert Klopfleisch

Institute of Veterinary Pathology
Freie Universität Berlin
Berlin, Germany

`robert.klopfleisch@fu-berlin.de`

Marc Aubreville

Technische Hochschule Ingolstadt
Ingolstadt, Germany

`marc.aubreville@thi.de`

Frauke Wilm*

Pattern Recognition Lab, Computer Sciences
Friedrich-Alexander-Universität
Erlangen-Nürnberg, Germany

`frauke.wilm@fau.de`

Christof A. Bertram

Institute of Pathology
University of Veterinary Medicine
Vienna, Austria

`christof.bertram@vetmeduni.ac.at`

Andreas Maier

Pattern Recognition Lab, Computer Sciences
Friedrich-Alexander-Universität
Erlangen-Nürnberg, Germany

`andreas.maier@fau.de`

Katharina Breininger

Department of Artificial Intelligence
in Biomedical Engineering
Friedrich-Alexander-Universität
Erlangen-Nürnberg, Germany

`katharina.breininger@fau.de`

Abstract

The successful registration of digitized microscopic images is required for many applications in digital pathology. In particular, the registration of specimens scanned by different slide scanning systems may be beneficial to transfer expert annotations from one image domain to another and thereby reduce labeling effort. We present an iterative approach to register microscopic specimens digitized with multiple scanning systems, aiming to compute an optimal global transformation for the images at highest resolution. For this purpose, an initial registration based on a down-scaled version of the images is followed by a patch-based iterative update scheme. We make use of the hierarchical structure of digitized whole slide images to gradually approximate the optimal transformation. By using kernel density estimation to weight local transformation estimates, the

influence of registration errors can be further mitigated. We validate our method on five histologic and five cytologic samples, each scanned with four different scanning systems. Furthermore, we perform first experiments on samples stained with different stain combinations. Our experiments demonstrate the potential of the proposed method for a variety of datasets and application fields.

1. Introduction

Registration of pathological whole slide images (WSIs) is an essential component of many diagnostic routines in digital pathology. Registration can be used to transfer pathologist annotations from one image domain to another both to fuse information and to reduce labeling effort. The images to be registered can, for instance, be stained with different biological markers which highlight different structural and functional information of the tissue. Com-

*equal contribution

mon stain combinations are hereby Hematoxylin & Eosin (H&E), which allows for a good differentiation between cell nuclei and surrounding tissue, and an immunohistochemical (IHC) stain suitable for highlighting specific tissue components. Tellez *et al.* [10], for instance, used a combination of H&E-stained and Phosphohistone-H3 (PHH3)-stained samples to generate annotated training data for mitosis detection with minimal manual labeling effort. The immunohistochemical marker PHH3 highlights cells that are undergoing mitosis, making them easier to detect than in H&E-stained slides. By registering WSIs of the original and washed and re-stained sections, the authors created a comparatively large dataset of annotated mitotic figures, which would otherwise have required a considerable amount of time and human expertise using manual annotations. For registration, Tellez *et al.* first determined a global translation vector by maximizing the 2-D cross-correlation of random image patches and then registered each mitotic figure separately to include individual local shifts. A related application for registration is the alignment of consecutive sections taken from a tissue block for cross-sectional observation or 3-D reconstruction. Furthermore, the registration of microscopic samples digitized with different scanning systems can be useful to train supervised machine-learning algorithms on images from multiple scanner domains and thereby make the algorithm independent of scanner-specific features, without having to re-label the slides for each scanner-domain individually. Over the last few years, this scanner-independence of algorithms has received increasing attention. The Mitosis Domain Generalization (MIDOG) challenge by Aubreville *et al.* [1], for instance, addressed the issue of scanner variations in the case of assessing the mitotic count.

Recently, several approaches for the registration of histological samples have been proposed which can be categorized into rigid and non-rigid transformation estimations. The Non-Rigid Histological Image Registration (ANHIR) challenge organized by Borovec *et al.* [2] addressed the issue of registering histologic samples stained with different dyes. Out of the challenge participants, the method by Lotz *et al.* [5] performed particularly well. Their registration pipeline consisted of three main steps, each of which further minimized the normalized gradient field (NGF) similarity metric. The initial rigid pre-alignment was further improved by an iteratively computed affine transformation. Finally, a B-Spline transformation estimated a non-rigid registration. However, the registration was not evaluated on the original resolution, but on a down-scaled version of the WSIs. Due to their large size of up to ten billion pixels, these algorithms are most likely not applicable to WSIs at highest resolution. Especially for cytologic samples, however, a cell-accurate registration is required, which is not guaranteed by an estimation at lower resolution levels. The methods of the other participants of the ANHIR challenge were also mostly

based on classical image registration techniques. Only one team proposed a learning-based approach: For this purpose, the Volume Tweening Network by Zhao *et al.* [12], which was previously developed for 3-D medical image registration, was adapted to the data at hand. The network was first trained in an unsupervised manner with low resolution images and then optimized using the provided landmark positions of the training data. The advantage of this method is that it is comparatively fast. However, also in this case, the registration success was not evaluated on the original resolution. The use of landmarks introduced an additional bias and reduced the generalization ability [2]. Wodzinski and Müller [11] did not participate in the ANHIR challenge, but used the same dataset and achieved results comparable to the best scoring teams. The proposed deep learning-based, unsupervised method aimed to find the optimal displacement field in order to obtain a non-rigid registration. However, their results also indicated that the success of the registration can be highly dependent on the number of training samples of each tissue type for these data-driven approaches. Rossetti *et al.* [9] proposed a three-stage registration method to estimate a non-rigid transformation to reconstruct a 3-D tissue volume from serial tissue sections. An initial pre-alignment was estimated based on the principal axes of the contours, followed by a global similarity transformation and B-spline transformation to compensate for local tissue deformations. The final transformation was then propagated to high resolution layers. By only computing the transformation at a low resolution and then propagating the result to the highest resolution, this approach is highly dependent on an accurate estimation at the lowest level and bears the risk of error propagation. Furthermore, the initial pre-alignment using contours is only suited for histologic samples containing tissue architecture (such as surgical biopsies) and has limited applicability in the case of cytologic samples with individual (clusters of) cells. Mueller *et al.* [8] proposed a method for the non-rigid registration of adjacent tissue sections prepared with different stains. The two-step procedure first computed a B-spline deformable transform on low resolution images and then applied the pre-computed transformation to high-resolution patches. Similar to Rossetti *et al.*, this method bears the risk of error propagation.

In order to address this risk of error propagation Jiang *et al.* [4] recently proposed a hierarchical registration approach. They registered tissue sections that were stained with H&E, scanned and afterwards washed out and re-stained with a different marker. The authors argue that - due to the re-staining - a rigid transformation was sufficient to register the two scans. For their hierarchical registration Jiang *et al.* initially estimated a transformation using down-scaled versions of the WSIs. This initial transformation was used to extract corresponding image patches on all

resolution levels except for the original resolution. For each pair of patches, a translation vector was computed using a Fast Fourier Transform (FFT)-based approach. In order to minimize the influence of patches where the registration failed, the authors used kernel density estimation (KDE) to compute robust weights for the translation results. Finally, the offset for the original resolution level was estimated using hierarchical resolution regression. Even though the approach of Jiang *et al.* decreases the risk of error propagation by using hierarchical registration, the patch selection on each resolution level is only guided by the initial transformation computed at low resolution. We argue that even a small registration error at low resolution can have a high impact on the error during patch selection and, depending on the down-scaling factor for the initial registration, could for higher resolutions at worst magnify to a registration error larger than the patch size. This would result in patches that are completely disjoint and are not suited to perform a local registration. For this scenario even the KDE would not suffice to down-weight the influence of outliers as all selected patches will be affected by this phenomenon. In order to address this limitation, we alter the method by Jiang *et al.* to an iterative registration approach where we directly use the transformation estimated on a lower resolution level for the subsequent level estimate. Furthermore, we extend the method by incorporating rotation, anisotropic scaling and shear into the transformation estimation. Thereby, we enable the applicability to WSIs from varying scanning systems which do not necessarily use the same resolutions and magnification for digitization. We evaluated our approach using five histologic and five cytologic samples, each digitized with four different scanning systems, resulting in 40 WSIs. Furthermore, we conducted first experiments on five WSI-pairs prepared with different stain combinations. Overall, we showed a significant decrease of registration error compared to the original approach by Jiang *et al.* which is the only method natively applicable to WSIs where the code is publicly available. We provide access to our implementation on GitHub¹ and can provide access to the WSIs upon reasonable request.

2. Material

For our experiments we used three datasets for two different application fields. For the application of scanner invariance we used one histology dataset and one cytology dataset scanned with four different slide scanning systems: The Aperio ScanScope CS2 (resolution: $0.25 \frac{\mu\text{m}}{\text{px}}$), the Hamamatsu NanoZoomer S210 (resolution: $0.22 \frac{\mu\text{m}}{\text{px}}$), the Hamamatsu NanoZoomer 2.0 HT (resolution: $0.23 \frac{\mu\text{m}}{\text{px}}$) and the ZEISS Axio Scan.Z1 (resolution: $0.22 \frac{\mu\text{m}}{\text{px}}$). The histology dataset comprised five tissue-sections from canine

¹<https://github.com/DeepPathology/CrossScannerRegistration.git>

cutaneous mast cell tumors stained with H&E and the cytology dataset five equine bronchoalveolar lavage fluid samples stained with Prussian Blue. Although registering images from different scanning systems was the focus of our work, we also evaluated the applicability to images with different stainings. Our third dataset contained five H&E-stained colorectal cancer tissue samples. These samples were digitized using the Roche Ventana iScan HT scanner. After digitization, the H&E-stained slides were washed and re-stained with IHC and Hematoxylin counter stain.

2.1. Ground truth definition

Both registration scenarios, the registration of the same sample digitized with different scanning systems and the registration of the same sample stained with different dyes, in principal allow for a cell-accurate registration as the same cellular structure is shown on the fixed and the moving image. To quantitatively evaluate the registration results, we semi-automatically annotated landmarks on all images: We first used a regular 5×5 grid to equally distribute 25 landmarks on all WSIs. This equal distribution, however, can lead to landmarks being placed on ambiguous regions, e.g. background. Therefore, we used the online annotation software EXACT [7] to manually re-position these landmarks to descriptive image components in the immediate vicinity, e.g. tissue border components or cells. Using these landmarks, the registration error can be quantified by applying the estimated transformation to the landmarks of the transformed image and computing the mean euclidean distance to the landmarks of the fixed image.

3. Methods

For the main focus of our work, the registration of WSIs scanned with different slide scanning systems, we assume that an affine transformation is sufficient to register the images. Therefore, our method aims to find an optimal global transformation for the original image at highest resolution. We refer to this affine transformation matrix with six degrees of freedom as T . We adopted the hierarchical registration approach by Jiang *et al.* where the initial registration is estimated at a low resolution level and then followed by a patch-based registration to further refine the results. This procedure is illustrated in Figure 1.

By introducing an iterative approach and weighting the results using KDE, we enable a robust method to determine the final transformation parameters. More explicitly, our approach deviates from and extends the work of Jiang *et al.* as follows:

- adaptive matching of resolution levels to enable scanner-independence
- adaptive foreground detection to enable applicability to cytologic samples

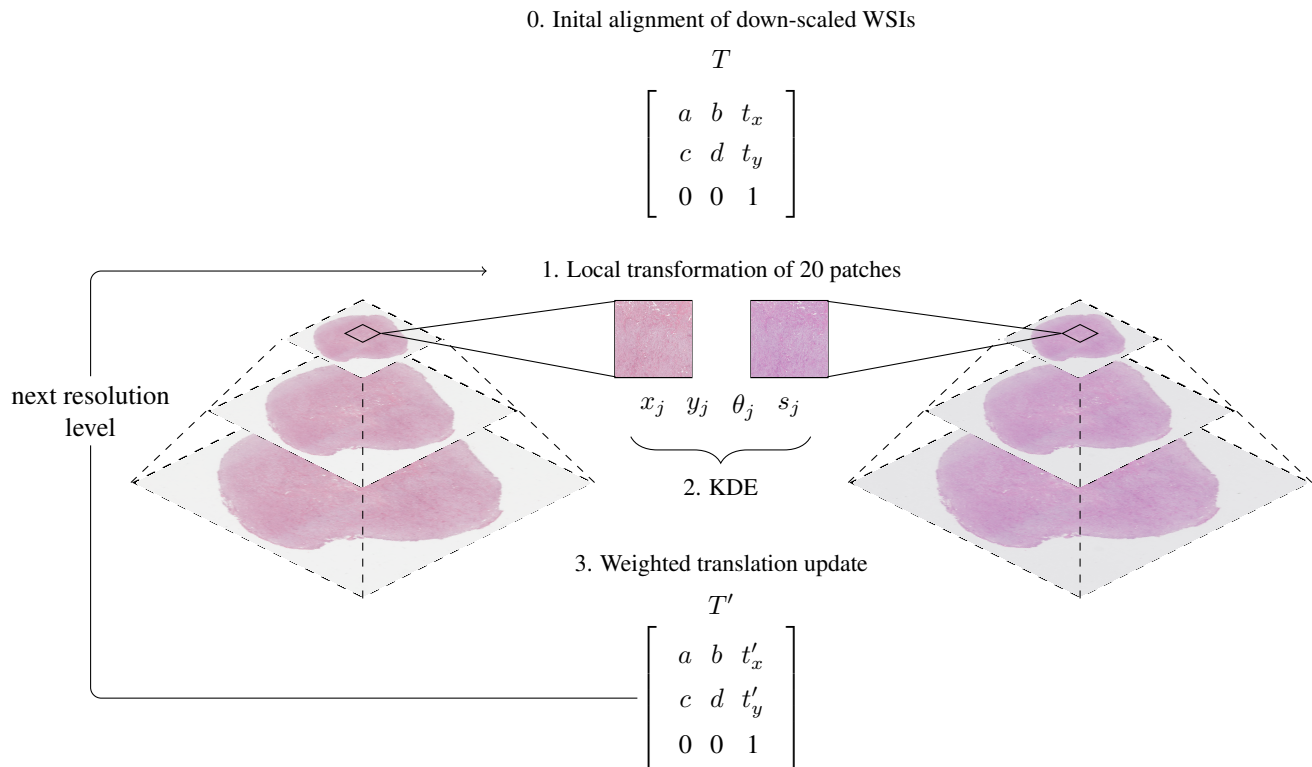


Figure 1: Illustration of overall registration pipeline. The initial registration is followed by an iterative update of the translation component. This is computed through a weighted sum of local translation updates. The corresponding weights are calculated using kernel density estimation (KDE) on all locally computed transformation parameters (translation x_j and y_j , rotation angle θ_j and scaling factor s_j). T : transformation matrix with components a, b, c, d as linear combinations of anisotropic scaling, rotation, and shearing and translation components t_x and t_y .

- incorporation of four additional degrees of freedom (due to rotation, anisotropic scaling and shearing) into the transformation matrix
- iterative update of the transformation matrix to enhance robustness of patch-selection

In the following sections, we will further elaborate on these contributions.

3.1. Registration process

To estimate the initial transformation, down-scaled thumbnails of the WSIs were used. For the results presented in this work, we used a down-scaling factor of 50 for all datasets. To allow pixel-level accuracy, the effective down-scaling factor in each dimension was chosen as integer division of the slide dimensions closest to the desired factor. An initial affine transformation matrix was determined by aligning landmarks computed with the Scale Invariant Feature Transform (SIFT) key-point extractor [6]. Due to the linear relationship across the WSI levels, an estimation of the translation vector at the original resolution

can be calculated by multiplying the result with the corresponding down-sampling factors. The scaling factors and the rotation angle, on the other hand, are independent of the resolution and can therefore be directly applied to higher resolution levels.

The initial global registration was followed by a patch-based local registration to further refine the parameters. For this purpose, 20 random image patches from the fixed WSI were sampled over several image levels. We used Otsu’s adaptive thresholding method to separate tissue components from non-informative background and constrained the patch selection to patches containing a certain percentage of tissue to ensure an adequate amount of tissue on the patch for a successful registration. This percentage threshold was initialized with 85% and successively lowered by 5% if no adequate patch was found for 25 iterations. Thereby, the method is also applicable to cytologic WSIs, which can contain a high amount of background pixels. For each patch from the fixed image, the corresponding patch in the moving image was computed using the initial transformation

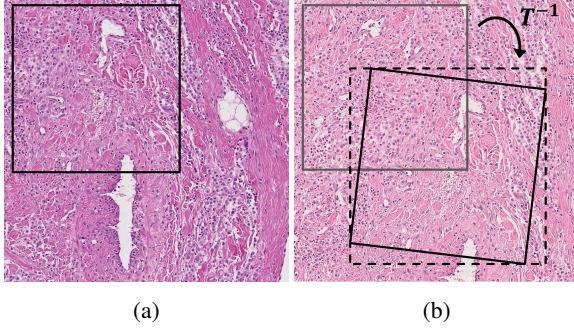


Figure 2: Visualization of the transformation process from the fixed WSI to the moving WSI: The black frame in (a) shows the patch in the fixed WSI. The gray frame in (b) depicts the same patch before the transformation in the moving WSI. By applying the transformation matrix T to the coordinates of the corner points, the resulting patch with the black frame in (b) can be determined. The surrounding dotted black frame is the bounding box and was used to extract the patch.

matrix. Since we limit our method to affine transformations, this can be achieved by applying the inverse transformation matrix to the coordinates of the vertices of the patch in the fixed slide. As the python OpenSlide² library does not allow the extraction of rotated patches, the bounding box of the transformed vertices was calculated and extracted. To obtain the final patch, the extracted region was then rotated in the opposite direction and cropped. This procedure is visualized in Figure 2. The resulting patches from both WSIs were registered once again using the FFT to optimize the final registration.

3.2. Iterative transformation estimation and KDE-weighting

As discussed previously, small errors of the translation vector are amplified as the resolution increases and can result in extracted patches with little or no overlap. For this reason, we propose an iterative procedure to increase the accuracy of the translation vector with each level. Starting at the lowest resolution level, 20 patches were extracted as described in Section 3.1 and registered using an FFT-based registration³. Registrations that resulted in rotation angles larger than 1° were excluded, as a large rotation angle indicates a failure of the local registration. The resulting local transformation parameters were used to compute an update of the initial registration.

To minimize the influence of patches where the registration failed, the results were weighted using KDE. KDE is

a non-parametric density estimator for modeling the underlying probability density function of a dataset. For an independent, identically distributed random sample $\vec{x}_1, \dots, \vec{x}_n \in \mathbb{R}^d$, KDE can be formally expressed as

$$\hat{f}_h(\vec{x}) = \frac{1}{nh^d} \sum_{i=1}^n K\left(\frac{\vec{x} - \vec{x}_i}{h}\right) \quad (1)$$

with $h = n^{-\frac{1}{d+4}}$ (Scott's Rule)

where $K : \mathbb{R}^d \mapsto \mathbb{R}$ is a non-negative kernel function and $h > 0$ is a smoothing parameter, the so-called bandwidth [3]. Like Jiang *et al.* we used a Gaussian kernel and defined the bandwidth by applying Scott's Rule. The resulting density estimates can be considered as a measure of confidence to weight the translation vectors. Thereby, the effect of registration errors can be mitigated by down-weighting their contribution to the final estimation.

We included all transformation parameters (translation, rotation and scaling) in the KDE estimation as they affect each other. We assume that using all parameters increases the robustness of the weight estimation. Let x_j, y_j, θ_j, s_j be the x -offset, y -offset, rotation angle and scaling factor of registering patch j at resolution level r , then the corresponding weight can be computed as:

$$w_j^r = \hat{f}_h(x_j, y_j, \theta_j, s_j). \quad (2)$$

Even though we obtained local parameters for translation, rotation and scaling, the affine representation does not allow an individual update of the latter two parameters. Therefore, whereas all of them were used during KDE to compute the update weights, only the translation component of the estimated transformation was updated before repeating the procedure at the next higher resolution level. To reduce the influence of patches where the registration failed, we only used the translation vectors of the ten patches with the highest KDE weights:

$$x^{r+1} = \sum_{j=1}^{10} \overline{w}_j^r x_j^r \quad y^{r+1} = \sum_{j=1}^{10} \overline{w}_j^r y_j^r, \quad (3)$$

where \overline{w}_j^r is the patch-weight normalized by the sum of the ten highest KDE-results. Following this iterative procedure, we gradually approached the final transformation.

4. Evaluation and results

A series of experiments were conducted to evaluate the proposed method. As described in Section 2.1 we semi-automatically annotated landmarks on all images. By applying the estimated transformation to the landmarks of the moving image and computing the mean euclidean distance to the landmarks of the fixed image, we could quantitatively

²<https://openslide.org>

³<https://imreg-dft.readthedocs.io>

evaluate the accuracy of the registration. The registration process was repeated three times per slide and registration errors were averaged across repetitions to verify the reproducibility of the results. Mean and standard deviation were then calculated across all five slides for each scanner combination. These results are summarized in Table 1 for the histology dataset in Table 2 for the cytology dataset. While the mean reflects the accuracy of the registration, the standard deviation indicates the robustness of our method to inter-slide variations such as slide quality and artifacts.

The proposed method performed well on both datasets for scanner invariance. For the histology dataset the results ranged between 1.23 μm and 7.99 μm (Table 1). On the cytology dataset the proposed method performed well for all scanner combinations. The mean registration error varied between 2.36 μm and 4.65 μm (Table 2). For comparison: The average radius of neoplastic mast cells is approximately 6 μm , which indicates a cell-accurate registration for most cases. The checkerboard overlay in Figure 3 of two exemplary patches allows the direct visual evaluation and demonstrates the success of the registration.

The first column of Tables 1 and 2 states the optimal transformation error when using the annotated landmarks to compute an affine transformation. The third column summarizes the registration error when directly applying the initial transformation computed at down-scaled thumbnails of the WSIs. The results show that for both datasets, the iterative update of the translation vector generally led to an improvement of the registration. For the histology dataset, we additionally compared our approach to the original method by Jiang *et al.* In order to allow a fair comparison, we adapted the method by Jiang *et al.* to take into account scaling differences between the fixed and moving image as we used slides from varying scanning systems which do not necessarily use the same resolutions and magnification factors for digitization. The results in Table 1 clearly show that our approach is able to outperform this method. In their publication, Jiang *et al.* argued that re-stained tissue has a relatively fixed position on the slide and thus the transformation can be estimated as a rigid transformation. Since we have a similar scenario where the same slides are scanned by different slide scanning systems, one could assume that this also holds for our samples. We explain the large discrepancies between the method of Jiang *et al.* and our approach by different stitching behaviors of the slide scanners which can introduce non-isotropic scaling factors as well as minor differences in slide placement between repeated scans which can cause rotation angles that are not negligible. Therefore an affine matrix is better suited to estimate these transformations.

Due to an intensity-based tissue detection method, the approach of Jiang *et al.* failed for the registration of slides from the cytology dataset. By using an adaptive thresh-

olding for tissue detection as described in Section 3.1, our method is applicable to this dataset and performed exceptionally well for all scanner pairs.

The proposed method did not perform as well for the task of registering slides with different stainings. Table 3 summarizes the results when applying the methods to the re-stained slides. For two of the slides, the approach by Jiang *et al.* failed, even though it was designed for this application. For one of these slides (row 4) our iterative update scheme failed because all local patch registrations resulted in rotation angles significantly larger than 1° and were excluded from KDE-estimation leaving no parameters to compute the update. In these rare cases our implementation returned the initial transformation estimate. Figure 4 visualizes the slides corresponding to the third row in Table 3, which resulted in the highest registration error. It can be seen that the tissue was significantly affected by the re-staining process resulting in large tissue folds or detached tissue. These artifacts significantly influence the initial registration, which cannot be compensated by merely updating the translation. Nevertheless, for all examples, our method results in smaller registration errors than the approach by Jiang *et al.*

5. Discussion and outlook

In this work, we presented a method for registering WSIs scanned by different slide scanning systems. For this purpose, we have adapted the method by Jiang *et al.*, which only estimates translation offsets, by including rotation and scaling parameters. Using an iterative method to update the translation vector and incorporating KDE directly in each update, we were able to outperform the results by Jiang *et al.*

Our experiments have shown that the initial registration was generally improved by iteratively updating the translation vector using local patch registration results on increasingly higher resolution levels. In future work, we plan to increase the accuracy of estimating rotation and scaling parameters in a similar fashion. By assuming an affine transformation, however, it is difficult to directly incorporate these values in the transformation matrix due to interactions between rotation, scaling and shearing. Furthermore, the FFT-based registration implementation that we used only results in an isotropic scaling factor, which might lead to inaccurate approximations. In future work, a similar approach to KDE has to be found to directly interpolate between local transformation matrices.

In this work we focused on the registration of slides digitized by different slide scanning systems. We were able to obtain reliable results for both the cytology and the histology dataset. Many works in the research area of WSI registration are based on elastic transformations. This is mainly attributed to the use of consecutive and re-stained slides.

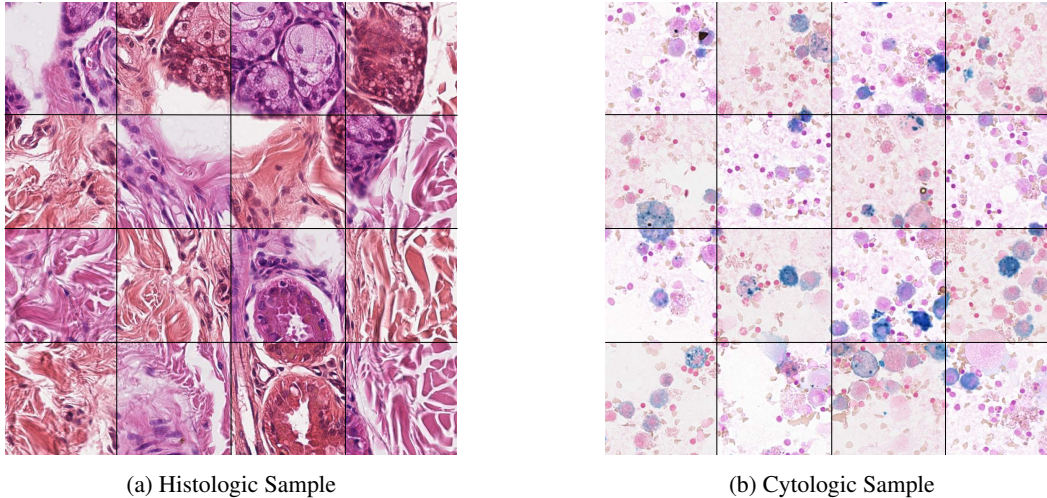


Figure 3: Two examples for the visual evaluation of the registration result. For visualization, the checkerboard technique was used which alternately stitches together a segment of the fixed image and the transformed moving image.

Scanner pair	Optimal	Mean registration error \pm standard deviation [μm]		
		Jiang <i>et al.</i>	Initial	Ours
CS2 / S210	0.79 ± 0.19	418.50 ± 592.70	3.54 ± 0.70	2.04 ± 0.31
CS2 / 2.OHT	0.92 ± 0.25	105.08 ± 97.26	3.71 ± 0.87	2.39 ± 0.63
CS2 / Z1	3.82 ± 6.50	206.34 ± 166.27	8.08 ± 11.09	8.25 ± 11.26
2.OHT / S210	0.83 ± 0.11	79.81 ± 79.60	1.20 ± 0.24	1.43 ± 0.20
Z1 / S210	3.81 ± 6.47	71.31 ± 64.82	9.51 ± 11.58	7.19 ± 11.59
Z1 / 2.OHT	3.90 ± 6.47	54.03 ± 28.47	8.93 ± 10.39	7.12 ± 11.88

Table 1: Mean registration errors and standard deviations [μm] of the histology dataset over three runs for slides from different scanner origins (fixed domain / moving domain). The result of our approach is compared to the optimal transformation, the method by Jiang *et al.* and our initial registration.

Both can result in severe changes of the tissue sample from slide to slide, making a non-rigid transformation necessary. In our case, however, one can assume the tissue sample is not manipulated by the re-scanning and the varying scanner properties mostly lead to affine transformations. We were only able to directly compare our results to the method of Jiang *et al.* as no other group provides an open source implementation of their method or only supports registration of down-sampled versions of the full-resolution WSIs. By providing access to our implementation on GitHub, we allow other researches to use the registration method for their own data and experiment with further refinement strategies for the final transformation estimation. Through an adaptive matching of resolution levels, our code is directly applicable to all combinations of slide scanning systems that are supported by the OpenSlide library. Furthermore, this work also incorporates cytologic samples in the registration evaluation. We assume that many approaches fail to register these images as they contain a high percentage of back-

ground pixels which can lead to failures of intensity-based pre-processing steps as could be seen for the approach of Jiang *et al.* By using an iterative adaptation of tissue detection, our method performs well on these images.

Moreover, we have already successfully applied our registration approach for the development of a segmentation algorithm that is robust across WSIs from different slide scanning systems. In this use case, the goal is to use an adversarial learning-based approach to constrain a segmentation network to learn a feature representation that is scanner-invariant. For this, the same tissue samples were scanned by two different slide scanning systems. However, only one dataset was annotated by a pathologist. Our registration approach allows us to transfer the annotations from one domain to another and thus obtain a labeled dataset for both domains.

The task of registering slides with different stainings highlights limitations of our approach. Due to detached tissue on re-stained slides, the initial estimation did not pro-

Scanner pair	Mean registration error \pm standard deviation [μm]			
	Optimal	Jiang <i>et al.</i>	Initial	Ours
CS2 / S210	1.10 ± 0.38	-	4.20 ± 2.92	3.61 ± 2.17
CS2 / 2.0HT	0.91 ± 0.64	-	5.25 ± 7.70	4.55 ± 6.38
CS2 / Z1	1.09 ± 0.82	-	3.19 ± 1.01	3.14 ± 0.94
2.0HT / S210	1.16 ± 0.40	-	2.14 ± 0.37	2.30 ± 0.65
CS2 / S210	1.46 ± 0.90	-	3.86 ± 2.05	3.68 ± 1.54
CS2 / 2.0HT	1.40 ± 0.92	-	2.41 ± 0.68	2.75 ± 0.55

Table 2: Mean registration errors and standard deviations [μm] of the cytology dataset over three runs for slides from different scanner origins (fixed domain / moving domain). The result of our approach is compared to the optimal transformation and our initial registration. The method of Jiang *et al.* failed to register the cytology samples.

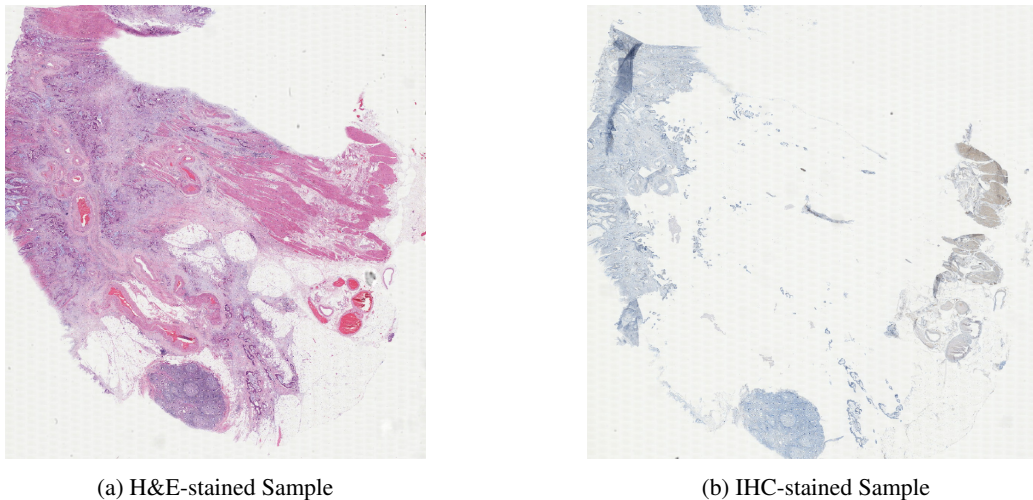


Figure 4: Sample pair heavily affected by detached tissue due to re-staining procedure.

Slide	Registration error [μm]			
	Optimal	Jiang <i>et al.</i>	Initial	Ours
1	2.69	68.39	18.96	13.33
2	3.37	17.89	17.07	12.58
3	22.86	-	46.55	47.46
4	2.73	-	10.47	10.47
5	2.02	37.28	31.62	14.29

Table 3: Mean registration error [μm] for re-stained slides. The result of our approach is compared to the optimal transformation, the method by Jiang *et al.* and our initial registration. The method of Jiang *et al.* failed for two slides.

vide a robust estimate and local patch registrations failed. In future work, strategies to adequately compensate for these registration failures have to be implemented. Furthermore, alternatives to the intensity-based FFT registration might increase the robustness of local transformations.

References

- [1] Marc Aubreville, Christof Bertram, Mitko Veta, Robert Klopffleisch, Nikolas Stathonikos, Katharina Breininger, Natalie ter Hoeve, Francesco Ciompi, and Andreas Maier. Mitosis domain generalization challenge. Zenodo, doi: [10.5281/zenodo.4573978](https://doi.org/10.5281/zenodo.4573978), 2021. 2
- [2] Jiří Borovec, Jan Kybic, Ignacio Arganda-Carreras, Dmitry V Sorokin, Gloria Bueno, Alexander V Khvostikov, Spyridon Bakas, Eric I-Chang Chao, Stefan Heldmann, et al. Anhir: automatic non-rigid histological image registration challenge. *IEEE transactions on medical imaging*, 39(10):3042–3052, 2020. 2
- [3] Yen-Chi Chen. A tutorial on kernel density estimation and recent advances. *Biostatistics & Epidemiology*, 1(1):161–187, 2017. 5
- [4] Jun Jiang, Nicholas B Larson, Naresh Prodduturi, Thomas J Flotte, and Steven N Hart. Robust hierarchical density estimation and regression for re-stained histological whole slide image co-registration. *PLOS ONE*, 14(7):e0220074, 2019. 2
- [5] Johannes Lotz, Nick Weiss, and Stefan Heldmann. Robust, fast and accurate: a 3-step method for automatic histological

- image registration. *arXiv preprint arXiv:1903.12063*, 2019. [2](#)
- [6] David G Lowe. Distinctive image features from scale-invariant keypoints. *International journal of computer vision*, 60(2):91–110, 2004. [4](#)
- [7] Christian Marzahl, Marc Aubreville, Christof A Bertram, Jennifer Maier, Christian Bergler, Christine Kröger, Jörn Voigt, Katharina Breininger, Robert Klopffleisch, and Andreas Maier. Exact: a collaboration toolset for algorithm-aided annotation of images with annotation version control. *Scientific Reports*, 11(4343), 2021. [3](#)
- [8] Dan Mueller, Dirk Vossen, and Bas Hulsken. Real-time deformable registration of multi-modal whole slides for digital pathology. *Computerized Medical Imaging and Graphics*, 35(7-8):542–556, 2011. [2](#)
- [9] Blair J Rossetti, Fusheng Wang, Pengyue Zhang, George Teodoro, Daniel J Brat, and Jun Kong. Dynamic registration for gigapixel serial whole slide images. In *2017 IEEE 14th International Symposium on Biomedical Imaging (ISBI 2017)*, pages 424–428. IEEE, 2017. [2](#)
- [10] David Tellez, Maschenka Balkenhol, Irene Otte-Höller, Rob van de Loo, Rob Vogels, Peter Bult, Carla Wauters, Willem Vreuls, Suzanne Mol, Nico Karssemeijer, et al. Whole-slide mitosis detection in h&e breast histology using phh3 as a reference to train distilled stain-invariant convolutional networks. *IEEE transactions on medical imaging*, 37(9):2126–2136, 2018. [2](#)
- [11] Marek Wodzinski and Henning Müller. Unsupervised learning-based nonrigid registration of high resolution histology images. In *International Workshop on Machine Learning in Medical Imaging*, pages 484–493. Springer, 2020. [2](#)
- [12] Shengyu Zhao, Tingfung Lau, Ji Luo, I Eric, Chao Chang, and Yan Xu. Unsupervised 3d end-to-end medical image registration with volume tweening network. *IEEE journal of biomedical and health informatics*, 24(5):1394–1404, 2019. [2](#)